

Locality-Aware Automatic Differentiation on the GPU for Mesh-Based Computations

AHMED H. MAHMOUD, Massachusetts Institute of Technology, USA
 JONATHAN RAGAN-KELLEY, Massachusetts Institute of Technology, USA
 JUSTIN SOLOMON, Massachusetts Institute of Technology, USA

We present a high-performance system for automatic differentiation (AD) of functions defined on triangle meshes that exploits the inherent sparsity and locality of mesh-based energy functions to achieve fast gradient and Hessian computation on the GPU. Our system is designed around per-element forward-mode differentiation, enabling all local computations to remain in GPU registers or shared memory. Unlike reverse-mode approaches that construct and traverse global computation graphs, our method performs differentiation on the fly, minimizing memory traffic and avoiding global synchronization. Our programming model allows users to define local energy terms while the system handles parallel evaluation, derivative computation, and sparse Hessian assembly. We benchmark our system on a range of applications—cloth simulation, surface parameterization, mesh smoothing, and spherical manifold optimization. We achieve a geometric mean speedup of $6.2\times$ over optimized PyTorch implementations for second-order derivatives, and $2.76\times$ speedup for Hessian-vector products. For first-order derivatives, our system is $6.38\times$, $2.89\times$, and $1.98\times$ faster than Warp, JAX, and Dr.JIT, respectively, while remaining on par with hand-written derivatives.

CCS Concepts: • **Mathematics of computing** → **Automatic differentiation**; • **Computing methodologies** → **Massively parallel algorithms**; **Mesh geometry models**.

ACM Reference Format:

Ahmed H. Mahmoud, Jonathan Ragan-Kelley, and Justin Solomon. 2025. Locality-Aware Automatic Differentiation on the GPU for Mesh-Based Computations. In . ACM, New York, NY, USA, Article 111, 9 pages. <https://doi.org/XXXXXXX.XXXXXXX>

1 INTRODUCTION

Countless algorithms for science and engineering applications rely on a common building block: evaluating the gradient of a functional defined over a mesh. Gradient computation most often arises in optimization-driven tasks in physical simulation, inverse problems, design automation, and geometry processing. Each of these applications—and many others—can benefit from routines that evaluate gradients as seamlessly and efficiently as possible.

The prevalence of (stochastic) gradient descent methods in machine learning has led to a wide variety of efficient software tools for fast automatic differentiation (AD). Prior work in AD has been largely driven by the needs of machine learning where the dominant computational model involves *dense tensors*. Frameworks like PyTorch [Ansel et al. 2024] and JAX [Bradbury et al. 2018] are highly optimized for such workloads, enabling end-to-end differentiation of neural networks with *dense* computation graphs.

Conference acronym 'XX, June 03–05, 2018, Woodstock, NY

© 2025 Copyright held by the owner/author(s). Publication rights licensed to ACM. This is the author's version of the work. It is posted here for your personal use. Not for redistribution. The definitive Version of Record was published in , <https://doi.org/XXXXXXX.XXXXXXX>.

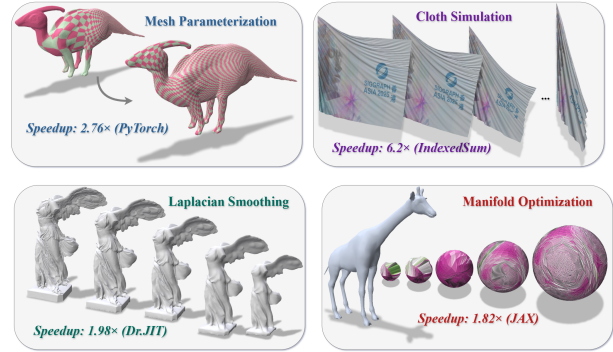


Fig. 1. Our system enables fast and flexible automatic differentiation (AD) of functions defined on triangle meshes by leveraging locality-aware forward-mode AD on the GPU. By confining all derivative calculations to registers and shared memory, we avoid the global memory bottlenecks associated with reverse-mode AD. Across a range of mesh-based tasks, we consistently outperform state-of-the-art AD frameworks, achieving substantial speedups in gradient, Hessian, and Hessian-vector product computations.

In contrast, scientific and graphics workloads—particularly those involving meshes—operate in a fundamentally different regime. Mesh-based problems often involve **large, sparse systems with localized dependencies and irregular topology**. These problems are characterized by complex sparsity patterns derived from irregular mesh connectivity. As mesh resolution increases to meet accuracy demands in fields like biomechanics, structural engineering, and CFD, the resulting Jacobians and Hessians become large and sparse. Existing AD frameworks—optimized for dense tensor operations—fail to exploit this structure. As a result, they suffer from poor runtime performance and excessive memory usage when applied to mesh-based problems. This inefficiency makes AD a major bottleneck—sometimes outweighing even the cost of solving the associated linear systems (see inset). Thus, practitioners are forced to limit resolution, avoid second-order methods, or handcraft derivatives to maintain performance [Huang et al. 2024].

Mesh-based problems thus demand AD systems that natively exploit sparsity, avoid dense intermediate representations, and scale

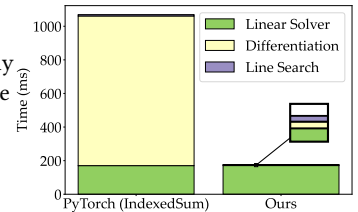


Fig. 2. Prior to our system, nonlinear optimization using Newton's method (mass-spring systems here) was bottlenecked by differentiation. Our system significantly accelerates derivative computation, shifting the bottleneck to the linear solver.

to millions of variables while handling irregular topologies. While some mesh-specific AD frameworks have been proposed (see §3.2), they are either CPU-based—failing to leverage the massive parallelism of modern GPUs—or limited to first-order derivatives.

AD in mesh-based computations on the GPU is fundamentally memory-bound—the primary cost lies not in arithmetic operations but in repeatedly accessing and updating large, sparse data structures. On modern GPUs, achieving high performance requires careful navigation of the memory hierarchy where GPU registers and shared memory offer far greater bandwidth and lower latency than global memory. However, the irregularity and sparsity of access patterns make it difficult for conventional AD systems to exploit this hierarchy effectively.

In this paper, we present a high-performance AD system tailored to the sparsity and locality of mesh-based computations. Our key insight is that **differentiation on meshes is inherently local**—each gradient or Hessian contribution depends only on a small neighborhood around a mesh element. We exploit this structure to confine differentiation entirely to fast, on-chip GPU memory, reducing global memory traffic (see Figure 3). Our system uses forward-mode AD via operator overloading to compute per-element derivatives independently. By organizing computations around mesh *patches* and precomputing sparsity patterns, we avoid dynamic graph construction and maximize memory throughput.

In this paper, we make the following contributions ¹

- A GPU-efficient AD system for triangle meshes that outperforms existing frameworks (e.g., PyTorch, JAX, Warp, and Dr.JIT) in both speed and memory usage by leveraging the local structure of mesh energy functions and aligning computations with the GPU memory hierarchy.
- An intuitive programming interface designed for geometry processing and simulation workloads.
- A suite of benchmark applications including mass-spring cloth simulation, mesh parameterization, manifold optimization, and mesh smoothing demonstrating the performance advantages of our approach against various state-of-the-art baselines.

2 BACKGROUND

We briefly review the two main modes of AD as they are central to the rest of the paper. For a more comprehensive treatment, we refer readers to the textbooks by Naumann [2012] and Griewank and Walther [2008].

AD is a family of techniques to compute derivatives of functions expressed as computer programs. AD exploits the fact that any such program is a composition of elementary operations with known derivatives allowing for systematic application of the *chain rule*. There are two primary modes of AD: *forward* and *reverse mode*.

In forward mode, derivatives propagate from inputs to outputs, computing the directional derivative of a function $f : \mathbb{R}^n \rightarrow \mathbb{R}^m$ along a chosen tangent direction. Forward mode maintains a derivative (or dual) value alongside each intermediate variable during program execution. A common implementation strategy is operator overloading where each arithmetic operation is redefined to also

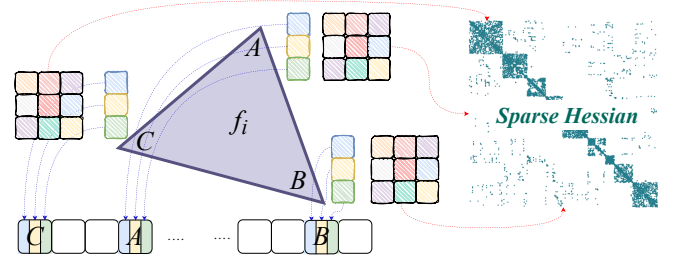


Fig. 3. Per-element derivative computation and assembly. For a local energy term f_i over triangle ABC , we compute derivatives with respect to local variables (in \mathbb{R}^3) using compact indexing. We evaluate gradients and Hessians in registers/shared memory as small dense vectors/matrices via forward-mode AD, then we map them to global indices and accumulate them into the global gradient or sparse Hessian.

compute and propagate the derivative. This approach aligns naturally with the execution order of the original program—each node carries forward both its value and its local derivative.

In reverse mode, derivatives are propagated from outputs to inputs, computing the gradient of a scalar-valued function $f : \mathbb{R}^n \rightarrow \mathbb{R}$ by traversing the computation graph in reverse. Reverse mode requires first recording a computation graph during the forward pass which captures all intermediate variables and dependencies. During the reverse pass, this graph is traversed backward to apply the chain rule and accumulate gradients with respect to the inputs.

3 RELATED WORK

We categorize existing AD systems into two broad groups. The first includes general-purpose, domain-agnostic systems that can be applied to any problem as long as it is expressed within the framework’s programming model. The second group consists of domain-specific framework, designed specifically for geometric data processing, and in particular, for computations on meshes.

3.1 AD Tools

ADOL-C [Griewank et al. 1996] is a foundational C/C++ library that computes gradients and higher-order derivatives using operator overloading and taping. While broadly applicable, its tape management introduces runtime overhead and limits compiler optimizations, making it less suited for performance-critical tasks. PyTorch [Ansel et al. 2024] and JAX [Bradbury et al. 2018] are more recent AD systems that are widely used in machine learning and numerical computing with efficient support for dense tensor operations. However, their execution models are less effective for sparse, irregular structures or fine-grained control flow typical in scientific computing and geometric data processing.

Enzyme [Moses et al. 2021, 2022] performs AD at the LLVM IR level, enabling compiler-level optimizations that reduce memory and execution overhead—especially in reverse mode. This makes it attractive for integrating AD into existing high-performance codebases. Enoki [Jakob 2019] is a C++17 library that supports forward and reverse-mode AD with vectorized execution across CPU and GPU. Dr.JIT [Jakob et al. 2022], its successor, compiles high-level

¹The source code for our system and applications is available at <https://github.com/owensgroup/RXMesh>

Python/C++ code into optimized machine code, enabling efficient differentiable rendering. While effective in rendering contexts, both systems are limited to first-order derivatives and do not exploit the sparsity or locality common in mesh-based computations. Our system builds on the insights behind these tools, adapting them to better suit sparse workloads in mesh processing—leading to improved performance in our target domain.

3.2 Mesh AD Tools

Herholz et al. [2022] proposed a system that applies symbolic differentiation to unoptimized C++ code operating on sparse data. Their approach constructs a global expression graph across the mesh, eliminates redundant subexpressions, and generates vectorized, parallel kernels for CPU or GPU execution. While this yields highly optimized code, it incurs high memory usage and long compilation times. To address these issues, Herholz et al. [2024] introduced a refinement where users define symbolic expressions for a single mesh element. The system compiles these element-wise kernels independently of the global mesh, significantly reducing memory usage and compile times.

TinyAD [Schmidt et al. 2022] is a C++ library designed for sparse optimization. It computes gradients and Hessians by differentiating small, per-element subproblems. Users define local energy terms and the system applies forward-mode AD to compute first- and second-order derivatives. While structurally similar to our method, TinyAD runs only on CPUs and uses OpenMP for parallelism. Our work builds on TinyAD’s structure but is designed explicitly for GPUs by optimizing for memory locality and parallel throughput.

Opt [Devito et al. 2017] is a DSL for nonlinear least squares problems. It uses symbolic differentiation at the IR level and generates first-order optimization code. Thallo [Mara et al. 2021] extends Opt by improving scheduling and memory layout. Unlike our system, these systems focus specifically on least squares problems and do not generalize to broader mesh computations. Warp [Macklin 2022] is a Python-based framework for high-performance spatial computing. Users write simulation kernels in Python which are JIT-compiled for CPU or GPU. Warp supports reverse-mode AD by generating backward kernels enabling simulation differentiation and integration with ML pipelines.

In summary, while several mesh-based AD tools support GPU execution, many overlook the importance of memory locality. Some focus solely on symbolic simplification [Herholz et al. 2024, 2022], or lack higher-order derivatives (e.g., Opt, Thallo, Warp), and some run only on the CPU [Schmidt et al. 2022]. In contrast, our method treats the GPU as a first-class target and optimizes all AD operations with an emphasis on memory locality and execution efficiency.

4 LOCALITY IN MESH-BASED AUTOMATIC DIFFERENTIATION

In this work, we target a broad class of mesh-based problems where *the objective function decomposes into a sum of local energy terms*. These problems are common in simulation, optimization, and geometric data processing and share a key property: the objective is *partially separable* [Nocedal and Wright 2006], meaning it can be

expressed as a sum of functions, each depending only on a small subset of the variables.

4.1 Problem Overview

Formally, we differentiate an energy function $F : \mathbb{R}^n \rightarrow \mathbb{R}$ of the form

$$F(x) = \sum_{j \in \mathbb{E}} f_j(x_j), \quad (1)$$

where \mathbb{E} denotes a set of mesh elements (e.g., vertices, edges, or faces), and each $f_j : \mathbb{R}^{k_j} \rightarrow \mathbb{R}$ is a localized energy term associated with the j element. Here, k_j denotes the number of degrees of freedom influencing f_j —typically determined by the mesh element’s local neighborhood. The vector $x \in \mathbb{R}^n$ encodes the global degrees of freedom. Each f_j depends only on a small set of variables (x_j) selected from x —typically the degrees of freedom associated with element j and its immediate neighbors.

This local dependency is conveniently captured by a binary *selection matrix* $S_j \in \{0, 1\}^{k \times n}$ such that $x_j = S_j x$. Differentiation distributes over summation, allowing us to compute per-element gradients $g_j \in \mathbb{R}^{k_j}$ and Hessians $H_j \in \mathbb{R}^{k_j \times k_j}$ independently. These local derivatives are then assembled into global structures via

$$g = \sum_{j \in \mathbb{E}} S_j^\top g_j \quad \text{and} \quad H = \sum_{j \in \mathbb{E}} S_j^\top H_j S_j. \quad (2)$$

For functions defined over a mesh, computing per-element gradients (g_j) and Hessians (H_j) exhibits strong *locality*—each local energy term $f_j(x_j)$ depends only on a small neighborhood around the corresponding mesh element j . For example, when computing energy contributions for a triangle, only the positions of its three vertices are involved. Consequently, the local gradient $g_j \in \mathbb{R}^{k_j}$ and Hessian $H_j \in \mathbb{R}^{k_j \times k_j}$ remain small and bounded for most cases, e.g., edges are only connected to two vertices. This sparsity and locality makes per-element differentiation both tractable and highly parallelizable. The only global operation is the summation in Equation 2 which can be efficiently implemented using standard parallel reduction primitives on the GPU [NVIDIA Corporation 2025].

4.2 Forward-mode vs. Reverse-mode AD

Reverse-mode AD is *asymptotically* more efficient than forward-mode when computing derivatives of functions with many inputs and few outputs, as the cost of backward passes scales with the number of outputs [Martins and Ning 2021]. This advantage underlies its widespread adoption in most modern AD frameworks which target (scalar) loss functions in machine learning.

However, reverse mode is *practically* ill-suited for GPU-based mesh computations. The key reason is that mesh workloads are typically *memory-bound*, not compute-bound—evaluating $f_j(x_j)$ and its derivatives involves relatively few floating-point operations but many memory accesses. In addition, local gradients g_j and Hessians H_j are functions of only small sets of the inputs extracted by the selection matrix S_j (see Figure 4). As a result, the asymptotic advantage of reverse-mode AD does not hold in this context. Moreover, reverse-mode AD requires constructing and traversing a global computation graph in reverse which necessitates storing a large number of intermediate values during the forward pass. On GPU

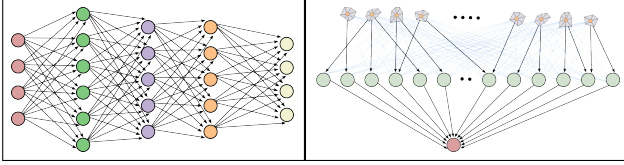


Fig. 4. A typical network in machine learning workloads exhibits dense connectivity across many layers resulting in high arithmetic intensity and making reverse-mode AD a suitable choice (left). In contrast, mesh-based problems give rise to shallow, sparsely connected computation graphs (right) where each local function depends only on a small subset of inputs. This structure makes forward-mode AD more efficient for the GPU execution.

architectures, this often means writing/reading to slow global memory. While checkpointing [Griewank and Walther 2008] can reduce memory usage, it introduces recomputation and synchronization overhead and does not alleviate reliance on global memory.

We posit that forward-mode AD is better suited to our setting. When computing local derivatives g_j and H_j , the number of inputs is small, making forward-mode and reverse-mode *theoretically* comparable in cost. However, forward-mode has the advantage that it does not require building or traversing a global computation graph. Instead, derivatives can be computed element-by-element *on the fly*, without global synchronization. This observation allows us to confine all necessary data—inputs, derivatives, and temporary values—to high-bandwidth on-chip memory (registers and shared memory) avoiding the overhead of global memory traffic.

5 OUR SYSTEM

In this section, we present our locality-aware AD system for triangle meshes. We begin by outlining the programming model that defines the user-system interaction (§5.1), followed by a detailed description of the system’s internal design and the low-level optimizations employed to maximize its performance (§5.2).

5.1 Programming Model

Our programming model is inspired by RXMesh [Mahmoud et al. 2021] and TinyAD [Schmidt et al. 2022]—combining their strengths in mesh-centric access and element-wise differentiation. Users define mesh-based objectives in a natural and declarative way by writing local energy terms over mesh elements while the system handles derivative tracking, memory management, and parallel execution. As shown in Listing 1, the user specifies the floating-point type, the variable dimension, and the type of mesh element the term operates on (Line 4). The core of the definition is a lambda function that computes the local energy for each element, taking in a handle to the element, an iterator over its neighborhood, and the optimization variables (Line 7). The return value is a scalar of type `ActiveT` which represents values being differentiated, i.e., active variables—as opposed to constants or auxiliary values which use standard floating-point types, i.e., passive variables. Active and passive variables can be freely mixed in energy computations and utility functions are provided for explicit conversion when needed.

```

1 using T = float;
2 Mesh mesh;
3 constexpr int VariableDim = 2;
4 Problem<T, VariableDim, VertexHandle, true>
   problem(mesh);
5
6 // Energy term
7 problem.add_term<Op::FV>(
8     [=](const auto& fh, //Face Handle
9         const auto& iter, //Face's vertices iterator
10        auto& objective) { //Objective
11
12         ActiveT res = ...; //Local energy implementation
13         return res;});
14
15 problem.eval_terms();
16 T f = problem.get_current_energy();
17 // Access the objective, gradient, and Hessian:
18 // problem.objective, problem.grad, problem.hess

```

Listing 1. Example use of our programming model. The user defines a local energy term over mesh elements (in this case, per face), specifies the required neighborhood access (`Op::FV` indicates that for each face F , the term accesses its vertices V), and relies on the system to handle all parallel evaluation and differentiation. The global energy, gradient, and Hessian are assembled automatically from local contributions.

Once the local energy term is defined, the system automatically applies it in parallel across the mesh and assembles the contributions into the global objective, gradient, and sparse Hessian. This interface supports multiple terms with different element types and neighborhoods allowing flexible composition of complex objectives.

5.2 System Design

System Overview. Our system takes as input a triangle surface mesh (possibly non-manifold) and a set of user-defined energy terms. We begin by constructing a mesh data structure that supports fast local queries (§5.2.1). This data structure—adapted from RXMesh [Mahmoud et al. 2021]—is generic and agnostic to the specific neighborhood access patterns required by the energy terms. Next, we allocate all necessary memory for the computation. This includes 1) mesh attributes declared by the user, e.g., vertex normals, and 2) global gradient buffer and sparse Hessian matrix, as specified by the `Problem` configuration (§5.2.4). We then launch one GPU kernel per energy term to evaluate the user-defined local energy and accumulate its derivatives in parallel (§5.2.2, §5.2.3). Finally, to compute the total energy $F(x)$ in Equation 1, we apply an efficient parallel reduction using CUB [NVIDIA Corporation 2025]. We now describe the key design decisions that underpin our system and explain the rationale behind each.

5.2.1 Localized Queries. We adopt the patch-based partitioning strategy introduced in RXMesh [Mahmoud et al. 2021] and later used in MeshTaichi [Yu et al. 2022] to enable efficient local computation on the GPU. The mesh is divided into small, independent *patches* that fit in shared memory, allowing local queries and derivative evaluations to run with minimal global memory accesses. This design reduces latency, promotes data reuse, and aligns with the GPU execution model by assigning one patch per thread block.

We use RXMesh’s patching algorithm and shared-memory layout with a target patch size of 512 faces.

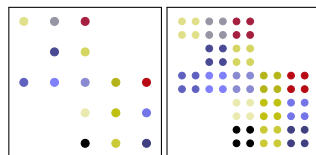
5.2.2 Local Derivative Computation. We implement forward-mode AD via operator overloading to compute per-element derivatives efficiently on the GPU. Each CUDA thread block collaboratively loads the patch’s input data (e.g., connectivity, attributes) from global memory once then performs all subsequent computations in registers or shared memory. Local energy terms are evaluated using a custom `ActiveT` type which wraps scalar values and tracks derivatives using compact local indexing. Internally, an `ActiveT` instance stores the primal value and its tangent (derivative) with respect to a small, fixed number of local variables. Arithmetic operations are overloaded to propagate these values according to the chain rule producing dense gradients and Hessians without requiring an explicit computation graph. For example, evaluating a triangle’s energy involves lifting its three vertex positions into `ActiveT`, propagating derivatives alongside values, and computing the resulting gradient $g \in \mathbb{R}^3$ and Hessian $H \in \mathbb{R}^{3 \times 3}$ directly in registers.

This one-pass approach avoids the memory and computational overhead of reverse-mode AD, which requires recording a computation graph during a forward pass and traversing it in reverse. Our method exploits the fixed, small number of variables per element—typical in mesh-based problems—and eliminates the need to materialize or store intermediate derivatives. Only the final global quantities (energy, gradient, Hessian) are written to memory.

5.2.3 Assembly. Once local derivatives have been computed, they are assembled into global gradient and Hessian matrices stored in global memory (Figure 3). Since multiple threads may attempt to update the same entries concurrently, race conditions can occur. One strategy to avoid such conflicts is graph coloring. However, in mesh-based problems, contention is typically low—each element interacts with only a small number of neighbors. Therefore, we rely on atomic operations for derivative accumulation. This approach simplifies implementation while maintaining high performance in practice. We evaluate the performance impact of this design choice in §6.4.

5.2.4 Sparse Hessian from the Mesh Topology.

A key advantage of mesh-based problems is that the sparsity pattern of the global Hessian is both structured and predictable. Each mesh element contributes n degrees of freedom, leading to a global Hessian of size $nM \times nM$, where M is the number of mesh elements and n is the dimension of the optimization variables. The nonzero blocks in this matrix follow the mesh adjacency: if two elements share a vertex—or participate in the same local energy term—they produce a dense $n \times n$ block in the Hessian (see inset). This structure is determined entirely by mesh connectivity and energy formulation.



Sparsity pattern of the Hessian (right) can be derived from the mesh sparsity—graph Laplacian here (left)—where each entry of the mesh graph is replaced by a dense block of size $n \times n$ where n is the dimension of the optimization variable.

We exploit this regularity to preallocate the Hessian in CSR format. During initialization, we analyze the mesh and the neighborhood access patterns declared in the `Problem` configuration (§5.1) to determine all potential element-element interactions. We run this analysis in parallel on the GPU and followed by a prefix-sum scan to compute global offsets and finalize allocation. When the user invokes `problem.eval_terms()`, we compute local Hessian contributions in parallel and accumulate them in the global matrix. This avoids dynamic memory allocation during execution, reduces runtime overhead, and improves GPU utilization.

5.2.5 Implicit Hessian-Vector Products. In addition to forming the full Hessian, our system supports implicit Hessian-vector products (HVPs)—often needed in optimization routines, e.g., Newton-CG. Instead of constructing the global matrix, we directly accumulate the result of applying each local Hessian to a user-specified input vector. This reuses the same infrastructure as Hessian assembly—we compute local derivatives in parallel, but rather than inserting $n \times n$ blocks into a global matrix, we apply them to slices of the input vector and atomically accumulate the result into an output vector. This eliminates the need to store the Hessian entirely and reduces both memory usage and runtime when only the product is required. Like global assembly, we run this operation as a parallel GPU kernel and we support all access patterns declared in the `Problem` definition. Users invoke it via `problem.hvp(x, v)`, where x is the current variable state and v is the input vector.

6 APPLICATIONS

We evaluate our system on four representative applications in mesh-based geometry processing and optimization, each highlighting a different capability or performance aspect. All experiments are conducted on an NVIDIA RTX 4090 GPU with 24 GB memory, using CUDA 12.6 on a system with an Intel® Core™ i9-14900KF (24-core, 4.4 GHz) and 64 GB RAM. Reported timings exclude preprocessing and data structure initialization.

In summary, mass-spring simulation (§6.1) evaluates gradient and sparse Hessian computation for second-order methods with multiple energy terms. Mesh parameterization (§6.2) tests our system’s ability to compute efficient Hessian-vector products in scenarios where explicit Hessian construction is unnecessary. Manifold optimization (§6.3) highlights the system’s flexibility in more complex tasks and benchmarks first-order derivative performance in the L-BFGS algorithm. Lastly, Laplacian smoothing (§6.4) serves as a first-order optimization benchmark comparing our gradient computation to various baselines and manual derivative implementation.

6.1 Cloth Simulation with Mass Spring Model

We start with a classical mass-spring system for cloth simulation where mesh edges act as springs and the system evolves under inertia and external forces [Provot 1995] (see Figure 1). Each timestep minimizes a composite energy consisting of inertial, elastic potential, and gravitational terms. Using implicit Euler integration [Li et al. 2024], we optimize the total energy:

$$E(x) = \frac{1}{2} \|x - (x^n + hv^n)\|_M^2 + h^2 P(x),$$

where x_d is the next vertex position, x^n, v^n are current positions and velocities, M is the lumped mass matrix, and h is the timestep.

The potential $P(x)$ includes:

- Spring energy: For edge $e = (i, j)$,

$$P_e(x) = l^2 \frac{1}{2} k \left(\frac{\|x_i - x_j\|^2}{l^2} - 1 \right)^2,$$

where x_i, x_j are the positions of the edge endpoints, l is the rest length, and k is a spring stiffness coefficient.

- Gravitational energy: $P_g(x) = -x^\top M g$, with g the constant gravity vector.

To optimize $E(x)$, we use Newton’s method with backtracking line search. Users define per-edge and per-vertex energies. Then, our system computes gradients and sparse Hessians automatically, solves the linearized system, and updates the solution. To improve robustness under large deformations, we apply *Hessian filtering* [Teran et al. 2005] by clamping negative eigenvalues to a small positive value, ensuring descent directions and stable convergence.

We compare our system to two alternative cloth simulation implementations, as summarized in Table 1.

PyTorch: In PyTorch, users define local energies as Python functions and compose the total energy via vectorized summation. We used (the reverse-mode) `autograd` and `torch.func.hessian` to compute the gradients and Hessians, respectively. While this supports AD out of the box, it produces *dense* Hessians, ignoring problem sparsity. By exploiting sparsity and GPU locality, our system achieves over two orders of magnitude speedup. As a consequence of PyTorch returning dense Hessians, Newton’s method relies now on dense Cholesky factorization, incurring significant memory overhead and poor scalability.

IndexedSum: To improve upon the naive PyTorch baseline, we compare against IndexedSum—a recent PyTorch-based library for sparse Hessian computation.² IndexedSum provides a lightweight wrapper around PyTorch `autograd` that constructs sparse Hessians from element-wise contributions using a gather-compute-scatter model. This approach closely mirrors our system: the user defines a local energy per element, and the framework automatically assembles the global energy, gradient, and sparse Hessian. While our work relies on forward-mode AD, IndexedSum performs a vectorized dense AD on the local Hessians using reverse-mode AD.

While IndexedSum reduces memory overhead and is significantly faster than naive PyTorch, it still incurs global memory traffic for local computations. In contrast, our system uses forward-mode AD, confines all computation to registers and shared memory, and performs only one global read (mesh data) and one write (gradients and Hessians). This architectural difference leads to a **6.2× speedup** over IndexedSum on meshes with $\approx 1M$ vertices.

6.2 Mesh Parameterization with Symmetric Dirichlet Energy

Our second application minimizes face-based distortion in mesh parameterization. The goal is to assign each 3D vertex a 2D coordinate (UV map) such that the mapping is as distortion-free as

²https://github.com/alecjacobson/indexed_sum

Table 1. Mass-spring performance. We report only the time per time step spent evaluating gradients and Hessians, excluding other components such as the linear solver. Results are averaged over 1000 time steps on meshes of varying sizes, identified by their number of vertices.

# V	PyTorch (ms)	IndexedSum (ms)	Ours (ms)
10^2	319.8	8.02	0.16
100^2	28004.6	9.07	0.24
500^2	OOM	21.9	3.58
1000^2	OOM	83.9	13.53

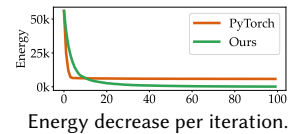
possible—critical for tasks like texture mapping, remeshing, and geometric modeling. We use the (area-scaled) symmetric Dirichlet energy [Smith and Schaefer 2015] which penalizes both stretching and shrinking of each triangle uniformly. Given a triangle mesh $\mathcal{M} = (\mathcal{V}, \mathcal{T})$ and a 2D map $x \in \mathbb{R}^{2|\mathcal{V}|}$, the objective is:

$$f(x) = \sum_{t \in \mathcal{T}} \text{area}_t \cdot \left(\|J_t(x)\|_F^2 + \|J_t(x)^{-1}\|_F^2 \right),$$

where $\|\cdot\|_F$ is the Frobenius norm, $J_t(x)$ is the 2×2 Jacobian of the affine UV mapping per triangle, computed as $J_t = [b - a \quad c - a] \cdot [b_r - a_r \quad c_r - a_r]^{-1}$, with a, b, c as UV coordinates and a_r, b_r, c_r the corresponding rest-pose 3D positions.

We implement this energy by defining a per-triangle energy term using our system. The user provides the local energy expression and our system computes the global energy, gradient, and (optionally) the Hessian. Minimization is performed using Newton’s method with line search (see Figure 7). Unlike the previous example, we avoid explicit Hessian assembly and adopt a matrix-free strategy. We use conjugate gradient (CG) requiring only Hessian-vector products. These are computed in our system by deriving localized per-element contributions without forming or storing the global Hessian.

For performance benchmark, we compare against a PyTorch implementation that computes Hessian-vector products using the *double backward* mechanism via `torch.autograd.grad`. This approach evaluates the directional derivative of the gradient by applying a second backward pass without explicitly forming the Hessian. Both implementations yield matching energy trajectories (see inset). Across various mesh resolutions, our system achieves a geometric mean **2.76× speedup** over PyTorch. This gain results from our design which avoids dynamic graph construction and reduces global memory traffic through localized computation.



6.3 Manifold Optimization

We implement spherical parameterization of a genus-0 triangle mesh by embedding it onto the unit sphere $\mathbb{S}^2 \subset \mathbb{R}^3$ while minimizing distortion and avoiding triangle flips [Schmidt et al. 2022]. Each vertex is represented as a point on \mathbb{S}^2 and optimization is performed in the 2D tangent space at each vertex. A retraction operator $R : \mathbb{S}^2 \times \mathbb{R}^2 \rightarrow \mathbb{S}^2$ maps updates back to the manifold. At each iteration, we compute the derivatives in tangent space, run one step of the solver, and update the tangent basis.

Table 2. Performance of the Newton solver using matrix-free Conjugate Gradient (CG). Instead of constructing the full Hessian, we compute Hessian-vector products on-the-fly during each CG iteration. The reported time is the average per Newton iteration. .

# V ($\times 10^6$)	PyTorch (s)	Ours (s)	Speedup
0.16	1.36	0.54	2.51 \times
0.56	4.57	1.74	2.62 \times
1.83	18.28	5.69	3.22 \times

The objective combines two terms: (1) a barrier function that penalizes flipped triangles, and (2) a stretch penalty encouraging uniform edge lengths. Formally, the objective is:

$$\min_{x \in \mathbb{R}^{2|V|}} \sum_{(i,j,k) \in F} \left[-\log \det([p_i, p_j, p_k]) + \|p_i - p_j\|^2 + \|p_j - p_k\|^2 + \|p_k - p_i\|^2 \right] \quad (3)$$

where each $p_i = R(s_i, x_i) \in \mathbb{S}^2$ is obtained by retracting a 2D tangent vector $x_i = [x_{i,1} \ x_{i,2}]^T \in \mathbb{R}^2$ at base point $s_i \in \mathbb{S}^2$ using a local orthonormal basis $b_{1,i}, b_{2,i} \in \mathbb{R}^3$. The retraction is defined as:

$$R(s_i, x_i) = \frac{s_i + x_{i,1} \cdot b_{1,i} + x_{i,2} \cdot b_{2,i}}{\|s_i + x_{i,1} \cdot b_{1,i} + x_{i,2} \cdot b_{2,i}\|}$$

We optimize the energy using L-BFGS with backtracking line search (see Figure 6). For comparison, we use JAXopt [Blondel et al. 2022], a JAX-based optimization library that also supports L-BFGS with backtracking line search. All JAXopt computations, including differentiation and linear algebra operations, are fully `jit`-compiled. Using the same configuration, on a mesh with 30k faces, our system achieves 0.88 ms/iteration, compared to JAXopt’s 1.57 ms/iteration, yielding a **1.78 \times speedup**. On a smaller mesh (Figure 1), we again reach 0.88 ms/iteration vs. 1.65 ms for JAXopt, a **1.87 \times speedup**. While JAX may better optimize the vector operations in L-BFGS, differentiation remains the dominant cost. This result highlights that our system maintains strong performance even in first-order methods—despite not targeting full linear algebra acceleration. In the next application, we isolate differentiation performance using pure gradient descent.

6.4 Laplacian Smoothing

This application demonstrates our system’s performance in first-order optimization through a simple geometric task: minimizing the sum of squared edge lengths, commonly known as *Laplacian smoothing* [Taubin 2012]. Given vertex positions $x \in \mathbb{R}^{3|V|}$, the energy is defined as: $E(x) = \sum_{(i,j) \in E} \|x_i - x_j\|^2$, where the sum is over mesh edges. This energy encourages neighboring vertices to stay close, effectively smoothing high-frequency noise. The gradient for vertex x_i is: $\frac{\partial E}{\partial x_i} = \sum_{j \in N(i)} (x_i - x_j)$, and optimization proceeds via gradient descent: $x_i \leftarrow x_i - \lambda \frac{\partial E}{\partial x_i}$, with step size $\lambda > 0$. While simplified—omitting cotangent weights and using explicit updates—this task typifies mesh-based optimization: computing local gradients and updating vertex positions.

We benchmark gradient computation against several AD frameworks: PyTorch and JAX (reverse-mode with JIT), Warp and Dr.JIT

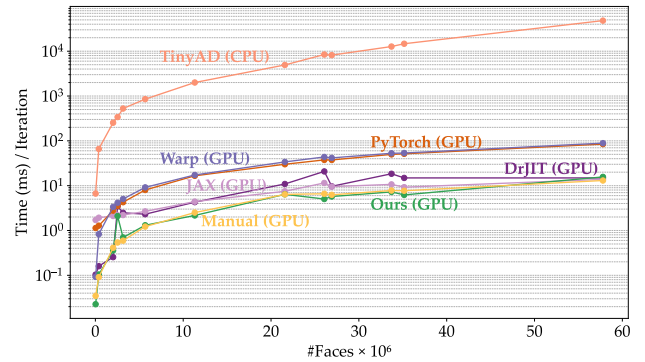


Fig. 5. Scaling performance of our system compared to GPU-based frameworks (PyTorch, Warp, Jax, and Dr.JIT), a manually implemented GPU baseline, and multithreaded CPU systems (TinyAD) on Laplacian smoothing application which requires gradient computations only.

(GPU-optimized reverse-mode), and a hand-coded baseline with closed-form gradients. Results in Figure 5 show that our system consistently outperforms CPU-based tools (e.g., TinyAD) and delivers strong GPU performance: **7.28 \times over PyTorch**, **6.38 \times over Warp**, **2.89 \times over JAX**, and **1.98 \times over Dr.JIT**. Compared to the manual baseline, we achieve a geometric mean speedup of 0.96 \times indicating our system incurs negligible overhead.

This result validates our use of atomic scatter for gradient accumulation. Although atomics are often associated with contention-related slowdowns, mesh-based workloads—Laplacian smoothing here—typically exhibit low write conflicts. The manual implementation uses a gather-based accumulation strategy, and the fact that both approaches yield similar performance further supports the effectiveness of scatter in this context.

7 CONCLUSION

Derivatives—especially Hessians—are expensive operations in general. However, on meshes, AD is inherently sparse and local. Our system takes advantage of this structure by confining per-element derivative computations to registers and shared memory, thereby avoiding global memory traffic and the overhead of global computation graphs. The result is an efficient and scalable AD system tailored to mesh-based applications. By aligning computation with the GPU memory hierarchy, our approach consistently outperforms state-of-the-art frameworks across a range of tasks in geometry processing and simulation.

Looking ahead, we plan to extend our system in several directions. First, we aim to support tetrahedral meshes in addition to triangle meshes. Second, our current design enforces strict locality—restricting access to immediate neighbors—to predict Hessian sparsity. We seek to relax this constraint. While the system currently assumes fixed, local support (e.g., one-ring neighborhoods), many practical workflows compose multiple local operations, effectively requiring wider k -ring support (e.g., the bi-Laplacian). Enabling such compositions while maintaining efficiency is a key direction for future work.

REFERENCES

- Jason Ansel, Edward Yang, Horace He, Natalia Gimelshein, Animesh Jain, Michael Voznesensky, Bin Bao, Peter Bell, David Berard, Evgeni Burovski, Geeta Chauhan, Anjali Chourdia, Will Constable, Alban Desmaison, Zachary DeVito, Elias Ellison, Will Feng, Jiong Gong, Michael Gschwind, Brian Hirsh, Sherlock Huang, Kshiteej Kalambarkar, Laurent Kirsch, Michael Lazos, Mario Lezcano, Yanbo Liang, Jason Liang, Yinghai Lu, CK Luk, Bert Maher, Yunjie Pan, Christian Puhersch, Matthias Reso, Mark Saroufim, Marcos Yukio Siraichi, Helen Suk, Michael Suo, Phil Tillet, Eikan Wang, Xiaodong Wang, William Wen, Shunting Zhang, Xu Zhao, Keren Zhou, Richard Zou, Ajit Mathews, Gregory Chanan, Peng Wu, and Soumith Chintala. 2024. PyTorch 2: Faster Machine Learning Through Dynamic Python Bytecode Transformation and Graph Compilation. In *29th ACM International Conference on Architectural Support for Programming Languages and Operating Systems, Volume 2 (ASPLOS '24)*. ACM. <https://doi.org/10.1145/3620665.3640366>
- Mathieu Blondel, Quentin Berthet, Marco Cuturi, Roy Frostig, Stephan Hoyer, Felipe Linares-López, Fabian Pedregosa, and Jean-Philippe Vert. 2022. Efficient and Modular Implicit Differentiation. In *Proceedings of the 36th International Conference on Neural Information Processing Systems (NIPS '22, Vol. 35)*. Curran Associates, Inc., Article 378, 13 pages. <https://doi.org/10.5555/3600270.3600648>
- James Bradbury, Roy Frostig, Peter Hawkins, Matthew James Johnson, Chris Leary, Dougal Maclaurin, George Necula, Adam Paszke, Jake VanderPlas, Skye Wanderman-Milne, and Qiao Zhang. 2018. *JAX: composable transformations of Python+NumPy programs*. <http://github.com/jax-ml/jax>
- Zachary Devito, Michael Mara, Michael Zöllhöfer, Gilbert Bernstein, Jonathan Ragan-Kelley, Christian Theobalt, Pat Hanrahan, Matthew Fisher, and Matthias Niessner. 2017. Opt: A Domain Specific Language for Non-Linear Least Squares Optimization in Graphics and Imaging. *ACM Trans. Graph.* 36, 5, Article 171 (Oct. 2017), 27 pages. <https://doi.org/10.1145/3132188>
- Andreas Griewank, David Juedes, and Jean Utke. 1996. Algorithm 755: ADOL-C: a package for the automatic differentiation of algorithms written in C/C++. 22, 2 (June 1996), 131–167. <https://doi.org/10.1145/229473.229474>
- Andreas Griewank and Andrea Walther. 2008. *Evaluating Derivatives: Principles and Techniques of Algorithmic Differentiation* (second ed.). Society for Industrial and Applied Mathematics, USA. <https://doi.org/10.5555/1455489>
- Philipp Herholz, Tuur Stuyck, and Ladislav Kavan. 2024. A Mesh-based Simulation Framework using Automatic Code Generation. *ACM Trans. Graph.* 43, 6, Article 215 (Nov. 2024), 17 pages. <https://doi.org/10.1145/3687986>
- Philipp Herholz, Xuan Tang, Teseo Schneider, Shoaib Kamil, Daniele Panozzo, and Olga Sorkine-Hornung. 2022. Sparsity-Specific Code Optimization using Expression Trees. *ACM Trans. Graph.* 41, 5, Article 175 (May 2022), 19 pages. <https://doi.org/10.1145/3520484>
- Zizhou Huang, Davi Colli Tozoni, Arvi Gjoka, Zachary Ferguson, Teseo Schneider, Daniele Panozzo, and Denis Zorin. 2024. Differentiable solver for time-dependent deformation problems with contact. *ACM Trans. Graph.* 43, 3, Article 31 (May 2024), 30 pages. <https://doi.org/10.1145/3657648>
- Wenzel Jakob. 2019. Enoki: structured vectorization and differentiation on modern processor architectures. <https://github.com/mitsuba-renderer/enoki>.
- Wenzel Jakob, Sébastien Speierer, Nicolas Roussel, and Delio Vicini. 2022. DRJIT: a just-in-time compiler for differentiable rendering. *ACM Trans. Graph.* 41, 4, Article 124 (July 2022), 19 pages. <https://doi.org/10.1145/3528223.3530099>
- München Li, Chenfanfu Jiang, and Zhaofeng Luo. 2024. *Physics-Based Simulation*. <https://phys-sim-book.github.io/>
- Miles Macklin. 2022. Warp: A High-performance Python Framework for GPU Simulation and Graphics. <https://github.com/nvidia/warp>. NVIDIA GPU Technology Conference (GTC).
- Ahmed H. Mahmoud, Serban D. Porumbescu, and John D. Owens. 2021. RXMesh: A GPU Mesh Data Structure. *ACM Transactions on Graphics* 40, 4, Article 104 (Aug. 2021), 16 pages. <https://doi.org/10.1145/3450626.3459748>
- Michael Mara, Felix Heide, Michael Zöllhöfer, Matthias Nießner, and Pat Hanrahan. 2021. Thallo – Scheduling for High-Performance Large-Scale Non-Linear Least-Squares Solvers. *ACM Trans. Graph.* 40, 5, Article 184 (Sept. 2021), 14 pages. <https://doi.org/10.1145/3453986>
- Joaquim R. R. A. Martins and Andrew Ning. 2021. *Engineering Design Optimization*. Cambridge University Press.
- William S. Moses, Valentin Churavy, Ludger Paehler, Jan Hückelheim, Sri Hari Krishna Narayanan, Michel Schanen, and Johannes Doerfert. 2021. Reverse-Mode Automatic Differentiation and Optimization of GPU Kernels via Enzyme. In *Proceedings of the International Conference for High Performance Computing, Networking, Storage and Analysis (St. Louis, Missouri) (SC '21)*. Association for Computing Machinery, New York, NY, USA, Article 61, 16 pages. <https://doi.org/10.1145/3458817.3476165>
- William S. Moses, Sri Hari Krishna Narayanan, Ludger Paehler, Valentin Churavy, Michel Schanen, Jan Hückelheim, Johannes Doerfert, and Paul Hovland. 2022. Scalable Automatic Differentiation of Multiple Parallel Paradigms through Compiler Augmentation. In *Proceedings of the International Conference on High Performance Computing, Networking, Storage and Analysis (Dallas, Texas) (SC '22)*. IEEE Press, Article 60, 18 pages. <https://doi.org/10.5555/3571885.3571964>
- Uwe Naumann. 2012. *The Art of Differentiating Computer Programs: An Introduction to Algorithmic Differentiation*. Society for Industrial and Applied Mathematics, Philadelphia, PA. <https://doi.org/10.1137/1.9781611972078>
- Jorge Nocedal and Stephen J. Wright. 2006. *Numerical Optimization (2 ed.)*. Springer New York, NY. <https://doi.org/10.1007/978-0-387-40065-5>
- NVIDIA Corporation. 2025. CUB: Cooperative primitives for CUDA C++. <https://nvidia.github.io/cccl/cub/>.
- Xavier Provot. 1995. Deformation Constraints in a Mass-Spring Model to Describe Rigid Cloth Behaviour. In *Proceedings of Graphics Interface '95 (Quebec, Quebec, Canada) (GI '95)*. Canadian Human-Computer Communications Society, Toronto, Ontario, Canada, 147–154. <https://doi.org/10.20380/GI1995.17>
- P. Schmidt, J. Born, D. Bommers, M. Campen, and L. Kobbelt. 2022. TinyAD: Automatic Differentiation in Geometry Processing Made Simple. *Computer Graphics Forum* 41, 5 (Oct. 2022), 113–124. <https://doi.org/10.1111/cgf.14607>
- Jason Smith and Scott Schaefer. 2015. Bijective Parameterization with Free Boundaries. *ACM Trans. Graph.* 34, 4, Article 70 (July 2015), 9 pages. <https://doi.org/10.1145/2766947>
- Gabriel Taubin. 2012. Introduction to Geometric Processing through Optimization. *IEEE Computer Graphics and Applications* 32, 4 (2012), 88–94. <https://doi.org/10.1109/MCG.2012.80>
- Joseph Teran, Eftychios Sifakis, Geoffrey Irving, and Ronald Fedkiw. 2005. Robust quasistatic finite elements and flesh simulation. In *Proceedings of the 2005 ACM SIGGRAPH/Eurographics Symposium on Computer Animation (Los Angeles, California) (SCA '05)*. Association for Computing Machinery, New York, NY, USA, 181–190. <https://doi.org/10.1145/1073368.1073394>
- Chang Yu, Yi Xu, Ye Kuang, Yuanming Hu, and Tiantian Liu. 2022. MeshTaichi: A Compiler for Efficient Mesh-based Operations. *ACM Transactions on Graphics* 41, 6, Article 252 (Nov. 2022), 17 pages. <https://doi.org/10.1145/3550454.3555430>

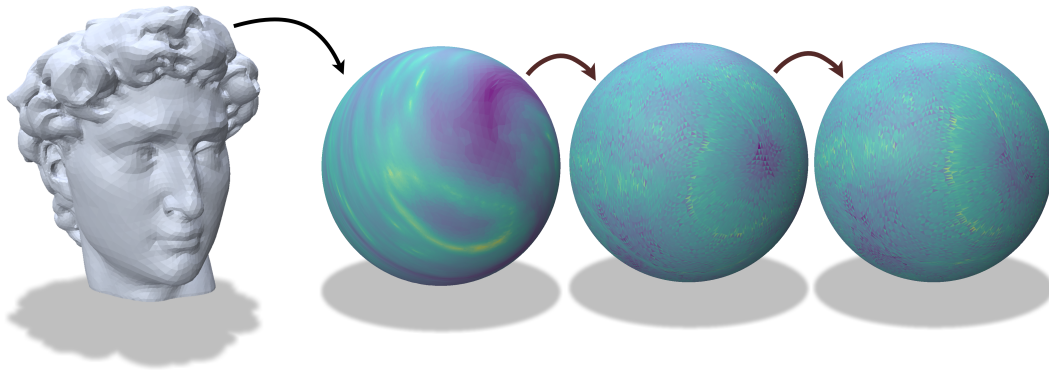


Fig. 6. Spherical parameterization of a genus-0 triangle mesh. From left to right: the input mesh, an initial mapping onto the unit sphere, an intermediate state during manifold optimization, and the final parameterization. Color encodes the local objective value at each face, highlighting distortion and injectivity terms (see Equation 3). The optimization iteratively reduces distortion while maintaining validity mapping.

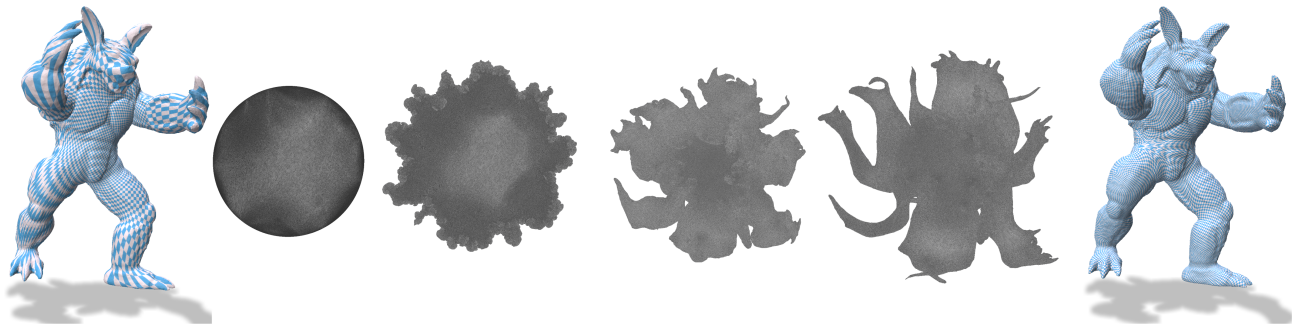


Fig. 7. Mesh parameterization using symmetric Dirichlet energy minimization. From left to right: the input mesh in 3D, the initial parameterization in UV space, and intermediate steps of the optimization showing progressive reduction in distortion, followed by the final parameterization mapped back to 3D. Our system performs this optimization using per-triangle energy terms and matrix-free sparse Hessian-vector products, achieving both efficiency and high-quality mappings.